X-SPECTRUM

White Paper

AEON
Event-Driven and Frame-Based X-ray Detector

Svenja C. Hövelmann, Jörn Lange, Alexandr Ignatenko, Dara Marin, Emanuele Besana, Stephan Stern, Andreas Beckmann, Sergej Smoljanin, Julian Schmehr, Jonas E. Warias

X-Spectrum GmbH

Hybrid pixel detectors operating in single-photon-counting mode have revolutionised X-ray science at synchrotrons and laboratory sources. The next generation of pixel readout chips, exemplified by the Timepix4 ASIC developed by the Medipix4 collaboration, overcomes the limitations of purely frame-based acquisition by making continuous, data-driven event streaming with sub-ns time stamping broadly accessible for synchrotron experiments. Here, we present the AEON detector system developed by X-Spectrum GmbH. AEON incorporates Timepix4 ASICs into a versatile multi-chip architecture with customisable sensor materials. The system operates either in frame-based mode or in event-driven mode, in which the Time-of-Arrival (ToA) and Time-over-Threshold (ToT) per pixel are recorded for each hit. We demonstrate benchmark results including resolved bunch filling patterns and highly efficient gate-free laser pump – X-ray probe experiments.

Table of contents

1. Introduction & Motivation **2**

2. AEON Detector Architecture & Key Features **3**

2.1 Hybrid Pixel Sensor Geometry and Modular Scalability *3*

2.2 In-Pixel Signal Processing and Readout Electronics *4*

2.3 Dual Data Acquisition Modes and Streaming Architecture *4*

2.4 Spectroscopic Capability, Multi-Photon Discrimination and Post-Processing Corrections *5*

3. Experimental Validation & Results **5**

3.1 Synchrotron Bunch Structure Timing and Background Filtering *5*

3.2 Gate-Free Laser Pump – X-Ray Probe Lattice Dynamics *6*

3.3 Dynamic Range Expansion *7*

4. Summary & Outlook **7**

5. Acknowledgement **8**

6. References **8**

1. Introduction & Motivation

The ongoing upgrade of synchrotron facilities worldwide to fourth-generation radiation sources — such as MAX IV[1], ESRF-EBS[2], SIRIUS[3], APS-U[4] — is dramatically increasing coherent X-ray brilliance and flux density and more fourth-generation radiation sources are under construction (HALF[5], HEPS[6]) and in planning (PETRA IV[7], BESSY III[8], Diamond-II[9]). Concurrently, advancements in ultrafast laboratory-based X-ray sources and high-repetition-rate free-electron lasers (FELs) demand detection systems capable of operating at the intersection of high spatial resolution, high photon flux, and sub-μs temporal resolution.

Over the past two decades, hybrid pixel detectors operating in single-photon-counting mode such as LAMBDA[10] (X-Spectrum GmbH) and EIGER2[11] (DECTRIS AG), have established the benchmark for X-ray diffraction and scattering experiments. However, conventional detectors operate primarily in frame-based acquisition modes. While effective for static or quasi-static measurements, frame-based architectures exhibit significant operational bottlenecks in time-resolved science.

In continuous frame-based measurements the time-resolution is typically limited to the ms range by the maximum frame rate. To probe μs down to the ns regime, as well as e.g. laser-shifted ps dynamics, the gating mode of the detector can be utilised. Yet only photons within a predefined narrow gate window are counted and photons arriving outside this window are discarded. Using this conventional gating setup, the experiment is blinded to intermediate states between pump pulses and any post-experiment realignment — such as correcting drifting window positions or evaluating multi-timescale relaxation dynamics. This leads to increased beamtime requirements and unnecessary sample radiation damage.

In contrast, event-driven detectors continuously record individual hits and create timestamped events with sub-ns time bins. By this, all out-of-window photons are retained, enabling flexible software-based post-gating. This allows for arbitrary temporal binning, offline correction of timing drifts, simultaneous ground-state tracking, and multi-timescale kinetic monitoring directly in post-processing, without data loss in time resolved

Published under a CC BY 4.0 licence
https://doi.org/10.5281/zenodo.22811176

experiments such as laser pump – X-ray probe studies[12].

Another advantage of the event-driven mode is the spectrometric information recorded for each hit, which facilitates the identification of chemical composition[13,14], increases image contrast in X-ray imaging[15,16], and supports beam-hardening correction algorithms in computed tomography[17]. In nuclear resonance scattering experiments, event-driven detectors raise the possibility to differentiate between instantaneous scattering and nuclear resonance processes on the ns timescale.

Furthermore, in sparse-signal experiments, such as diffuse scattering or dilute-sample X-ray photon correlation spectroscopy (XPCS)[18], event-driven data acquisition is superior to the classic frame-based mode in data-efficiency. Measuring in frame-based mode generates massive quantities of empty or zero-count pixel matrices and inundates downstream network and storage infrastructures. Meanwhile, event-driven detectors process individual photon interactions on-pixel and stream timestamped events with zero frame dead time reducing data volume.

A major milestone in the data-based and event-driven detector development is the Timepix4[19] ASIC, developed by the international Medipix4 collaboration hosted at CERN. Compared to its predecessor Timepix3[20], Timepix4 features an increased matrix size of 512×448 pixels with a pixel size of $55\,\mu m \times 55\,\mu m$, an increased theoretical readout bandwidth and most important, a drastically increased peak hit-rate capability of $3.6 \times 10^6\,ph/mm^2/s$ and $5 \times 10^9\,ph/mm^2/s$ in event-driven and frame-based mode, respectively.

Building upon the Timepix4 ASIC, X-Spectrum has developed the AEON detector, a versatile, large-area hybrid pixel detector designed for synchrotron and FEL beamlines, advanced laboratory instrumentation, and industrial applications. AEON bridges the gap between ultra-fast timing and high-throughput area detection and allows both event-driven and frame-based measurement modes. In the event-driven mode, continuous gate-free data streaming provides a $195\,ps$ time-bin resolution, achieving nanosecond-level time resolution with X-rays (see Section 3.1), while recording the pixel position, timestamp, and energy of each detected photon. In frame-based mode, frame rates up to 40 kHz and a dynamic range of 8-bit and 16-bit can be obtained.

Here, we report on the design, readout architecture, and experimental validation of the AEON detector system. We demonstrate its multi-modal capabilities through a series of benchmark experiments at leading synchrotron facilities, including bunch filling pattern identification, gate-free femtosecond laser pump – X-ray probe lattice dynamics and multi-photon hit detection.

2. AEON Detector Architecture & Key Features

2.1 Hybrid Pixel Sensor Geometry and Modular Scalability

The AEON detection system is engineered around a hybrid pixel architecture that couples a segmented semiconductor sensor substrate to the Timepix4 readout ASIC via flip-chip bump bonding. The sensor array features a square pixel matrix with a pixel size of $55\,\mu m \times 55\,\mu m$, ensuring high spatial resolution across the entire active detection area. To optimise quantum efficiency across a wide range of synchrotron and laboratory X-ray applications, AEON accommodates various sensor materials and thicknesses. For energies between 6 - $25\,keV$, silicon sensors are available in thicknesses of $300\,\mu m$ and $500\,\mu m$, offering near-unity absorption and minimal charge diffusion. For higher photon energies high-Z semiconductor materials are employed. Gallium arsenide (GaAs, $500\,\mu m$) provides high quantum efficiency in the 8 - $75\,keV$ regime, while cadmium telluride (CdTe, $1000\,\mu m$) and cadmium zinc telluride (CdZnTe, $2000\,\mu m$) extend the operational energy coverage from $8\,keV$ to $> 150\,keV$.

The system architecture scales from compact single-chip devices to tiled multi-module

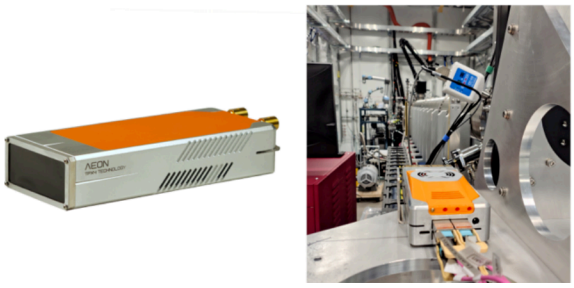


Figure 1 - Images of the AEON detector. Left: product image of the water cooled 700k model. Right: Air cooled 700k prototype used for the measurements at APS-U.

Published under a CC BY 4.0 licence
https://doi.org/10.5281/zenodo.22811176

assemblies. As an example, Figure 1 shows images of the AEON 700k detector. The single-chip AEON 230k configuration provides an active area of $24.6\,\text{mm} \times 28.2\,\text{mm}$ comprising 448×512 pixels. For larger detection areas, multi-chip modules such as the AEON 700k module ($74.4\,\text{mm} \times 28.2\,\text{mm}$, 1344×512 pixels) are used, while extended area configurations like AEON 2M, 7M, and 8.5M are built by tiling several of these modules into a multi-module geometry. The inter-chip gaps on a module are minimised to 2 pixels for high-Z and 4 pixels for Si sensors.

2.2 In-Pixel Signal Processing and Readout Electronics

Each pixel cell within the Timepix4 ASIC contains a complete analogue front-end and digital processing logic. The analogue chain consists of a charge-sensitive preamplifier with leakage current compensation, connected to a fast discriminator with a globally programmable and locally trimmable threshold voltage. When ionising radiation deposits charge above the preset threshold the Time-of-Arrival (ToA) and Time-over-Threshold (ToT) are measured. More details about the Timepix4 ASIC can be found in the Timepix4 publication[19].

The leading edge of the discriminator output latches the state of an internal time-to-digital converter, recording the ToA of the photon event. The on-chip time to digital converter delivers a temporal binning of $195\,\text{ps}$, which translates to a full-detector system timing resolution below $10\,\text{ns}$ for photons (see Figure 2a inset), limited by the varying absorption depth of photons inside the sensor, which leads to a varying arrival of the charge cloud at the pixelated electrodes. Thus, the achievable X-ray photon time resolution might improve further using electron-collecting Si or high-Z sensors with faster charge collection or Low-Gain-Avalanche Diodes.

Simultaneously to the ToA, the circuit measures the ToT, defined as the total duration that the preamplifier output voltage remains above the discriminator threshold. Because the discharge of the feedback capacitor occurs at a constant, controlled current, the measured ToT pulse width scales monotonically with the total charge deposited by the incident photon and thus the photon energy. The ASIC achieves a chip-level energy resolution of $1\,\text{keV}$, allowing per-pixel spectroscopic analysis without secondary pulse-height digitisers. Following each hit, the realisable pixel recovery time is governed by $\tau_{\text{dead}} = 400\,\text{ns} + \text{ToT}$, after which the pixel returns to a baseline state ready to register subsequent interactions.

2.3 Dual Data Acquisition Modes and Streaming Architecture

The AEON platform incorporates a dual-mode data acquisition architecture, allowing users to configure the detector in either a data and event-driven mode or a photon counting frame mode depending on beam flux and experimental requirements. In event-driven mode, the system functions as a continuous, asynchronous photon-streaming engine. Through autonomous on-chip sparsification, only pixels that register a charge deposit exceeding the discriminator threshold generate data packets. Each transmitted event packet contains four-dimensional coordinates consisting of the spatial position (X, Y), a ToA timestamp, and a ToT value. This mode eliminates global shutter clocks and frame-boundary dead time. In low-dose or diffuse-scattering regimes, this architecture drastically reduces data volume.

In frame-based mode, the detector operates as a single-photon counter. Hits are accumulated within local in-pixel counters across a user-defined exposure time. The counter depth can be configured to 8-bit or 16-bit depths on the hardware level, with extended 32-bit dynamic range supported via multi-framing firmware. In this mode, AEON will achieve continuous frame rates up to $40\,\text{kHz}$ with zero inter-frame dead time with the possibility of higher rates, handling local photon hit rates up to $5 \times 10^9\,\text{ph/mm}^2\text{/s}$ for high-intensity diffraction and imaging applications. In multi-module detector systems, these two operational schemes can be operated concurrently across different modules, either to simultaneously capture sparse diffuse scattering in event mode and intense Bragg peaks in frame mode, or to combine a global overview of structural scattering rings with high-speed, time-resolved tracking.

Being fully integrated into X-Spectrum's software library libxsp, AEON allows detector control and data acquisition by Python, C++ and REST API.

Published under a CC BY 4.0 licence
https://doi.org/10.5281/zenodo.22811176

2.4 Spectroscopic Capability, Multi-Photon Discrimination and Post-Processing Corrections

Because the event data stream natively retains spatial, temporal, and energy parameters for every recorded interaction, extensive analytical corrections can be performed in software post-processing.

When intense X-ray pulses generate multiple simultaneous interactions within the same pixel cell, standard single-threshold photon counters suffer from pulse pile-up and count losses. In the AEON system, the additive nature of charge deposition allows multi-photon events to be resolved within the ToT spectrum for a monochromatic beam. The calibrated energy histogram in Section 3.3 displays the possibility to extend the linear dynamic range of the detector well beyond traditional single-photon saturation limits.

Furthermore, charge sharing across adjacent pixels can be corrected using clustering of simultaneous, neighbouring hits. When a photon interaction occurs near a pixel boundary or when an escape peak due to the fluorescence of the sensor material occurs, the resulting charge cloud is divided among neighbouring pixels, producing multiple hits with split charge (and hence recorded energy). By identifying hit clusters occurring within a spatial radius of one pixel and a coincidence ToA window of e.g. $\Delta t < 10\,\text{ns}$, split charge packets can be recombined and assigned to the true primary coordinate, restoring spectroscopic integrity and suppressing spatial artifacts. In synchrotron timing experiments, software-level ToT filtering (such as rejecting events with $\text{ToT} < 30\,\text{ns}$) enables the suppression of substrate fluorescence and Compton scatter reducing inter-bunch baseline background signals to near zero without compromising the photometric yield of the primary beam.

3. Experimental Validation & Results

The event-driven and spectroscopic architecture of the Timepix4 ASIC enables a broad range of applications across synchrotron beamlines, free-electron lasers and high-energy radiation physics. Across the Timepix family, prominent experimental implementations encompass time-resolved Laue diffraction, X-ray emission and fluorescence spectroscopy, quantum optics coincidence counting, high-throughput computed tomography, multi-energy imaging, and dynamic coherent scattering. While the high spatial resolution and continuous timestamping capabilities of the AEON detector have also been demonstrated for ultra-fast X-ray Photon Correlation Spectroscopy (XPCS) resolving sample dynamics on sub-μs timescales, those comprehensive dynamic scattering results are reported in a separate dedicated publication.

In this work, we focus on the experimental validation of the AEON system through synchrotron bunch structure timing, gate-free laser pump–probe lattice dynamics, and multi-photon deconvolution.

3.1 Synchrotron Bunch Structure Timing and Background Filtering

The temporal performance of the AEON detector was assessed across multiple synchrotron radiation facilities operating under diverse storage ring filling patterns, including ESRF-EBS at European Synchrotron Radiation, APS-U at Argonne National Laboratory, PETRA III at Deutsches Elektronen-Synchrotron, and BESSY II at Helmholtz-Zentrum Berlin.

At ESRF-EBS beamline ID10-COH[21,22], timing measurements using monochromatic $9.6\,\text{keV}$ X-rays resolved the 7/8 + 1 filling pattern[23]. The multi-bunch-train spaced by $2.8\,\text{ns}$ fills 7/8 of the storage ring circumference and a cleaned single bunch is in the centre of the $352.3 \pm 0.3\,\text{ns}$ gap (see Figure 2a). For the single bunch an instrumental temporal resolution of $8.4 \pm 0.1\,\text{ns}$ FWHM was determined across the complete active sensor matrix (hole-collecting Si 300 μm) in continuous event-driven mode (see Figure 2a inset). Similar results were obtained by the non-commercial single-chip Timepix4 TEMPUS detector[24] developed independently by DESY.

The achieved time resolution permits individual electron bunches in storage rings to be cleanly separated without hardware shuttering.

At APS-U 8-ID-E,I, periodic bunch trains of the timing mode[4] with an average bunch spacing of $76.7 \pm 0.2\,\text{ns}$ were resolved (Figure 2b), while measurements at PETRA III beamline P10[25] identified the 40 bunch mode[26] structure with an average periodicity of $192.1 \pm 0.1\,\text{ns}$ (Figure 2c). The experimentally determined bunch spacings are

Published under a CC BY 4.0 licence
https://doi.org/10.5281/zenodo.22811176

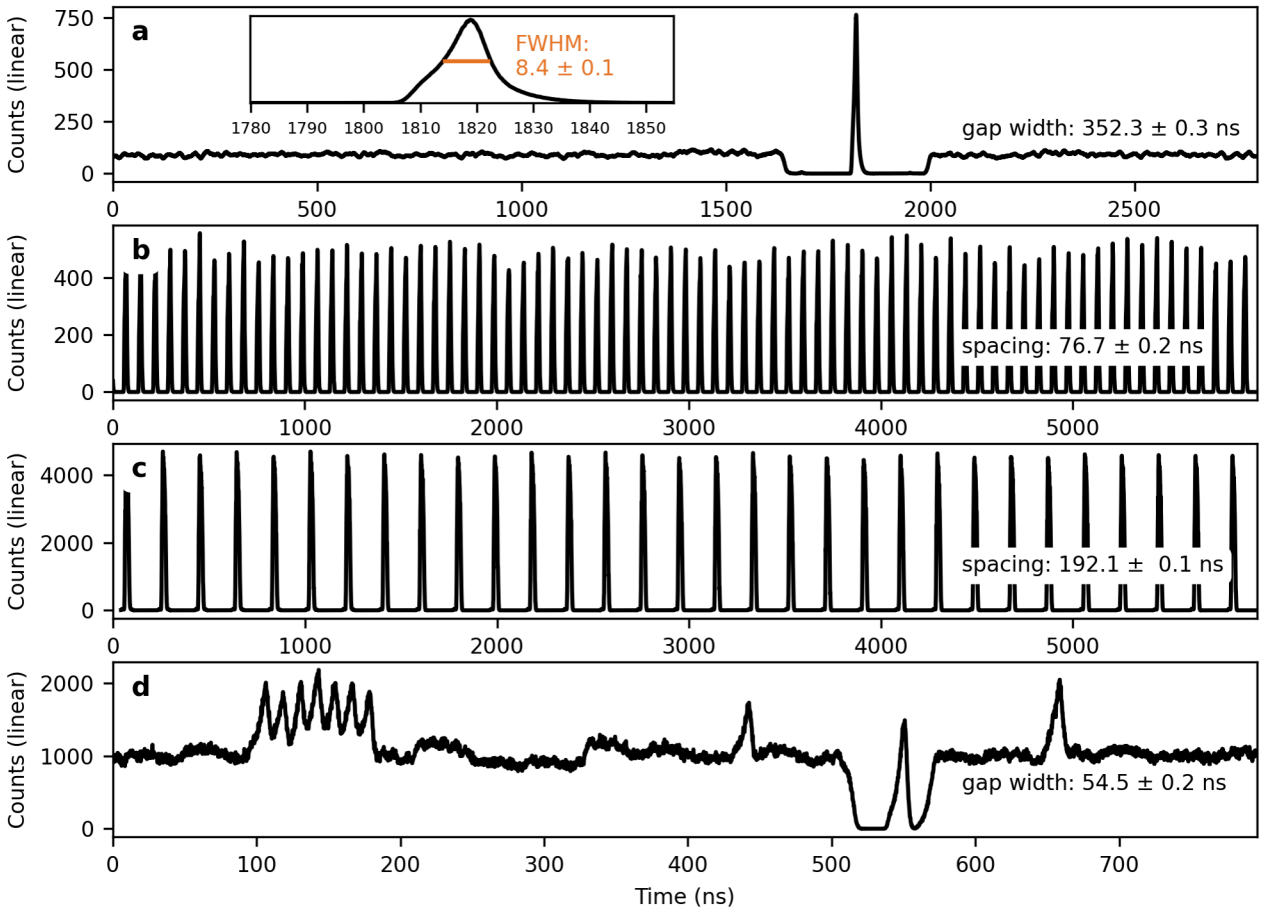


Figure 2 - Resolved bunch structures of different synchrotron filling patterns: (a) 7/8+1 bunch mode at ESRF-EBS, (b) timing mode APS-U, (c) 40 bunch mode at PETRA III and (d) multi bunch mode at BESSY II.

in good agreement with the theoretical bunch spacing in the corresponding storage ring operation modes.

Further, at BESSY II XPP@KMC-3[27] the complex multi-bunch filling pattern was characterised separating isolated single bunches, slicing pulses, and pulse-picking resonant excitation modes on top of multi-bunch-trains within the storage ring orbit (Figure 2d). The measurement verified the asymmetric gap spacing surrounding the single bunch with high signal-to-noise contrast and an observed total gap length of 54.5 ± 0.2 ns.

Because every event packet records the deposited energy through its ToT value, energy discrimination can be applied offline to suppress spurious background. Applying a software threshold cut for events with ToT < 30 ns selectively removes low-energy fluorescence and substrate scatter. This filtering suppresses the baseline signal between consecutive bunches to near zero while fully preserving the photometric intensity of the primary bunch peaks.

3.2 Gate-Free Laser Pump – X-Ray Probe Lattice Dynamics

Time-resolved diffraction measurements were conducted at BESSY II beamline XPP@KMC-3 to investigate ultrafast structural dynamics in epitaxial $SrRuO_3$ thin films grown on $SrTiO_3$ substrates. The sample was thermally excited using a femtosecond laser PHAROS (Light Conversion) emitting at $\lambda = 1028$ nm with a repetition rate of 104 kHz, corresponding to $1/12$ of the storage ring orbital revolution frequency and probed with monochromatic 8.7 keV X-rays. Optical absorption causes transient thermal lattice expansion, temporarily shifting the crystal lattice away from the Bragg diffraction condition, followed by thermal relaxation back to equilibrium across ns timescales. The dynamic behaviour was recorded utilising the event mode of the AEON detector to continuously detect individual photons while shifting the laser phase to scan the pump-probe delay (see Figure 3). During post-processing analysis, software

Published under a CC BY 4.0 licence
https://doi.org/10.5281/zenodo.22811176

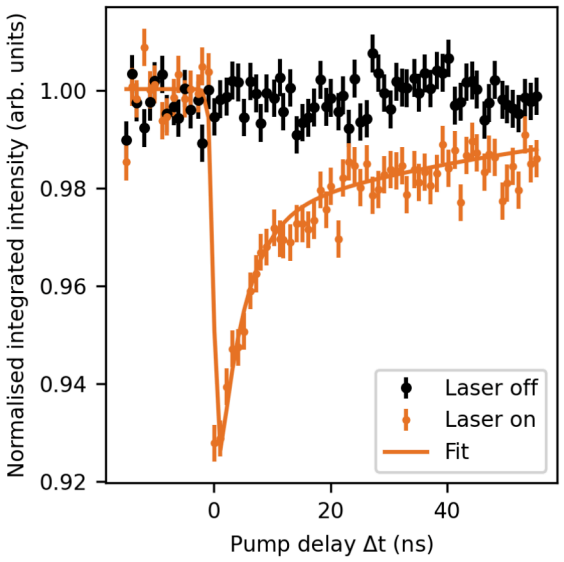


Figure 3 - Intensity of the SrRuO3 Bragg peak upon laser-induced thermal expansion and the following relaxation.

integration windows of approximately 30 ns were defined around the single bunch within the ring orbit. The pumped state exhibited a transient Bragg peak intensity reduction of 7.5 - 8% on the ps timescale followed by a recovery of the intensity on the ns timescale. The measured change in intensity and the observed timescales are in good agreement with previous studies[27] on the $SrRuO_3$ film. Because the laser excited the sample synchronously with only one specific orbital pass, the remaining 11 unpumped orbital passes within each orbit were recorded under identical beam conditions, serving as an internal normalisation reference that eliminated systematic errors from storage ring current decay and top-up injections, while simultaneously capturing longer relaxation times.

3.3 Dynamic Range Expansion

The per-pixel acquisition of spatial coordinates and ToT energy data enables energy-resolved transmission imaging without secondary hardware digitisers. In addition to spectral radiographic imaging, the spectroscopic capability of AEON provides a mechanism to extend the linear dynamic range under high-intensity illumination. In synchrotron exposures conducted at 12 keV X-rays at PETRA III beamline P10, the calibrated ToT spectrum resolved discrete peaks corresponding to single (1γ), double (2γ), and triple (3γ) photon absorption events occurring within a single pixel collection cycle (see Figure 4). By deconvolving

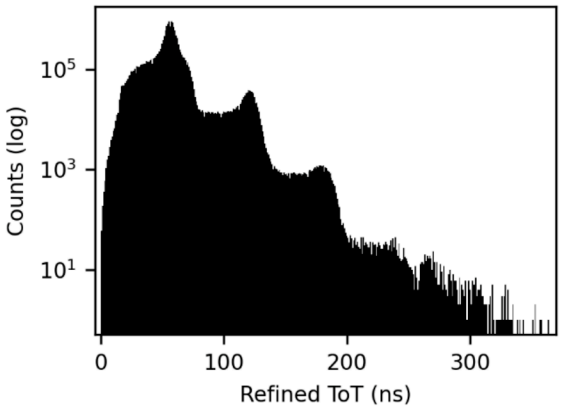


Figure 4 - ToT spectrum recorded at beamline P10, PETRA III showing the energy resolving capabilities and identification of multiphoton hits.

these multi-photon hits in software, quantitative photon counting is maintained beyond the pile-up saturation limits of conventional single-threshold counting architectures.

4. Summary & Outlook

The AEON detector represents a generational shift in hybrid photon-counting instrumentation. By integrating the Timepix4 ASIC architecture with a modular design and versatile selection of sensor materials, AEON bridges the gap between high-spatial-resolution 2D imaging and time-resolved kinetics in the ps, ns and sub-μs regimes. Its flexible dual-readout concept ensures full compatibility with established, high-throughput frame-based workflows — such as standard diffraction, scattering, and imaging experiments traditionally conducted with photon counting detectors while unlocking continuous, data-driven event streaming on the same physical platform. By eliminating the duty-cycle penalties, bandwidth inefficiencies, and delay-staging overhead inherent to conventional hardware-gated systems, AEON provides a universal detection platform tailored to the demands of fourth-generation diffraction-limited storage rings, FELs, advanced laboratory X-ray sources and industrial applications. Whether deployed for routine beamline operations, dynamic studies, gate-free pump–probe dynamics or energy-resolved spectroscopic imaging, the system sets a new standard for multi-dimensional X-ray science across fundamental and applied research.

Published under a CC BY 4.0 licence
https://doi.org/10.5281/zenodo.22811176

5. Acknowledgement

This work was supported by the Hamburgische Investitions- und Förderbank (IFB Hamburg).
Further, we thank the Medipix4 collaboration for support.

We acknowledge DESY (Hamburg, Germany), a member of the Helmholtz Association HGF, for the provision of experimental facilities. Parts of this research were carried out at PETRA III. Data was collected using beamline P10 operated by DESY Photon Science. We would like to thank Fabian Westermeier and Daniel Weschke for assistance during the experiments. Beamtime was allocated for beamtime ID 11023941.

We acknowledge the European Synchrotron Radiation Facility (ESRF) for provision of synchrotron radiation facilities under beamtime ID blc16590 and on beamline ID10-COH. We thank Marco Cammarata and Yuriy Chushkin for assistance and support during the beamtime.

Research parts were performed on APS beam time award (DOI: 10.46936/APS-191748/60015480) from the Advanced Photon Source, a U.S. Department of Energy (DOE) Office of Science user facility operated for the DOE Office of Science by Argonne National Laboratory under Contract No. DE-AC02-06CH11357. We thank Qingteng Zhang, Sam Marks, Suresh Narayanan, Eric Dufresne, Tejas Guruswamy and Miaoqi Chu for assistance and support during the beamtime.

Measurements were carried out at the XPP@KMC-3 beamline at the BESSY II electron storage ring operated by the Helmholtz-Zentrum Berlin für Materialien und Energie. We thank the Helmholtz-Zentrum Berlin für Materialien und Energie for the allocation of synchrotron radiation beamtime and Matthias Rössle and Florin Boariu for assistance during the experiment.

6. References

1. Tavares, P. F. *et al.* Commissioning and first-year operational results of the MAX IV 3 GeV ring. *J. Synchrotron Radiat.* **25**, 1291–1316 (2018).
2. Raimondi, P. *et al.* Commissioning of the hybrid multibend achromat lattice at the European Synchrotron Radiation Facility. *Phys. Rev. Accel. Beams* **24**, 110701 (2021).
3. Liu, L., Murilo Alves, Oliveira, A. C., Resende, X. & De Sá, F. Sirius Commissioning Results and Operation Status. in *Proc. IPAC'21* 13–18 (JACoW Publishing, Geneva, Switzerland, 2021).
4. Calvey, Joseph *et al.* Operation of the APS-U injectors with high single bunch charge. in *Proc. NAPAC2025* 20–25 (JACoW Publishing, Geneva, Switzerland, 2026).
5. Hu, L. *et al.* Design of a Test Beamline at Hefei Advanced Light Facility. *Photon Sci.* (2026).
6. Conroy, G. World's brightest X-rays: China first in Asia to build next-generation synchrotron. *Nature* **629**, 740–740 (2024).
7. Baev, K. *et al.* X-Ray Science at DESY: Upgrade Programs for the User Facilities FLASH and PETRA III. *Synchrotron Radiat. News* **37**, 4–11 (2024).
8. Viefhaus, Jens *et al.* BESSY III - status and overview. in *Proc. IPAC'23* 457–460 (JACoW Publishing, Geneva, Switzerland, 2023).
9. Ghasem, H., Kraljevic, N. B., Singh, B. & Martin, I. P. S. Lattice design for the Diamond-II light source storage ring. *Phys. Rev. Accel. Beams* **27**, 110704 (2024).
10. Pennicard, D. *et al.* Development of LAMBDA: Large Area Medipix-Based Detector Array. *J. Instrum.* **6**, C11009 (2011).
11. Donath, T. *et al.* EIGER2 hybrid-photon-counting X-ray detectors for advanced synchrotron diffraction experiments. *J. Synchrotron Radiat.* **30**, 723–738 (2023).
12. Chung, S., Vonk, V., Pennicard, D., Graafsma, H. & Stierle, A. Transient heating of Pd nanoparticles studied by x-ray diffraction with time of arrival photon detection. *Struct. Dyn.* **11**, 044301 (2024).
13. Genetay, T. *et al.* RQR beam qualities measurement with the Timepix4 detector. *Radiat. Meas.* **191**, 107570 (2026).
14. Delogu, P. *et al.* Validation of Timepix4 energy calibration procedures with synchrotron X-ray beams. *Nucl. Instrum. Methods Phys. Res. Sect. Accel. Spectrometers Detect. Assoc. Equip.* **1068**, 169716 (2024).
15. Procz, S. *et al.* X-ray and gamma imaging with Medipix and Timepix detectors in medical research. *Radiat. Meas.* **127**, 106104 (2019).

Published under a CC BY 4.0 licence
https://doi.org/10.5281/zenodo.22811176

16. Dudak, J. High-resolution X-ray imaging applications of hybrid-pixel photon counting detectors Timepix. *Radiat. Meas.* **137**, 106409 (2020).
17. Schuetz, M. K. *et al.* Optimized data acquisition for spectroscopic CT with Timepix3: combining photon-counting and data-driven readout modes with adaptive pixel masking. *J. Instrum.* **20**, P10045 (2025).
18. Chushkin, Y. *et al.* Achieving nanosecond time resolution with a two-dimensional X-ray detector. *J. Synchrotron Radiat.* **32**, 1220–1227 (2025).
19. Llopart, X. *et al.* Timepix4, a large area pixel detector readout chip which can be tiled on 4 sides providing sub-200 ps timestamp binning. *J. Instrum.* **17**, C01044 (2022).
20. Poikela, T. *et al.* Timepix3: a 65K channel hybrid pixel readout chip with simultaneous ToA/ToT and sparse readout. *J. Instrum.* **9**, C05013 (2014).
21. Chushkin, Y. *et al.* Three-dimensional coherent diffractive imaging on non-periodic specimens at the ESRF beamline ID10. *J. Synchrotron Radiat.* **21**, 594–599 (2014).
22. Jankowski, M. *et al.* The complex systems and biomedical sciences group at the ESRF: Current status and new opportunities after extremely brilliant source upgrade. *Nucl. Instrum. Methods Phys. Res. Sect. B Beam Interact. Mater. At.* **538**, 164–172 (2023).
23. Revol, Jean-Luc *et al.* Operation of the ESRF-EBS light source. in *Proc. IPAC'23* 449–452 (JACoW Publishing, Geneva, Switzerland, 2023).
24. Correa, J. *et al.* TEMPUS, a Timepix4-based system for the event-based detection of X-rays. *J. Synchrotron Radiat.* **31**, 1209–1216 (2024).
25. Zozulya, A. V. *et al.* Microfocusing transfocator for 1D and 2D compound refractive lenses. *Opt. Express* **20**, 18967–18976 (2012).
26. Keil, J., Sahoo, G. K., Schaumann, M. & Wanzenberg, R. PETRA III Operational Performance and Availability in 2023. *J. Phys. Conf. Ser.* **3010**, 012030 (2025).
27. Rössle, M. *et al.* The time-resolved hard X-ray diffraction endstation KMC-3 XPP at BESSY II. *J. Synchrotron Radiat.* **28**, 948–960 (2021).

Published under a CC BY 4.0 licence https://doi.org/10.5281/zenodo.22811176